SHEAR STRENGTHENING OF CONTINUOUS REINFORCED CONCRETE T-BEAMS USING WIRE ROPE UNITS

Keun-Hyeok Yang[a], Hang-Yong Byun[b], and Ashraf. F. Ashour[c]

[a] *Corresponding author, Department of Architectural Engineering, Mokpo National University, Mokpo, Jeonnam, South Korea.*

[b] *Korea Engineering & Consultant, Inc., Hwasun ,Jeonnam, South Korea.*

[c] *EDT1, School of Engineering, Design and Technology, University of Bradford, Bradford, BD7 1DP, UK.*

Biography: K. H. Yang is an assistant professor at Mokpo National University, Korea. He received his MSc and PhD degrees from Chungang University, South Korea. His research interests include ductility, recycling, strengthening, plasticity and shear of reinforced eco-friendly concrete structures.

H. Y. Byun is a chief at Korea Engineering & Consultant, Inc., South Korea. He received his MSc degree from Chonnam National University, South Korea. He is interested in the strengthening methods of concrete structures.

A.F.Ashour is a senior lecturer at the University of Bradford, UK. He obtained his BSc and MSc degrees from Mansoura University, Egypt and his PhD from Cambridge University, UK. His research interests include shear, plasticity, repair, strengthening and optimisation of reinforced concrete and masonry structures.

ABSTRACT

A simple unbonded-type shear strengthening technique for reinforced concrete beams using wire rope units is presented. Ten two-span reinforced concrete T-beams externally strengthened with wire rope units and an unstrengthened control beam were tested to failure to explore the significance and shortcomings of the developed unbonded-type shear strengthening technique. The main parameters investigated were the type, amount and prestressing force of wire rope units. All beams tested failed owing to significant diagonal cracks within the interior shear span. However, beams strengthened with closed type wire rope units exhibited more ductile failure than the unstrengthened, control beam or those strengthened with U-type wire rope units. The diagonal cracking load and ultimate shear capacity of beams with closed-type wire rope units were linearly increased with the increase of vertical confinement stresses in concrete owing to the prestressing force in wire rope units, while those of beams with U-type wire rope units were little influenced. It was also observed that average stresses in closed-type wire ropes crossing diagonal cracks at ultimate strength of beams tested were far much higher than those in U-type wire rope units, showing better utilization in case of closed-type wire ropes. The shear capacity of beams with closed-type wire rope units is conservatively predicted using the equations of ACI 318-05 for shear modified to account for the external wire rope units. A numerical formula based on the upper bound analysis of the plasticity theory is also developed to assess the load capacity of continuous T-beams strengthened with wire rope units. Comparisons between measured and predicted shear capacities showed that the coefficient of variation obtained from the mechanism analysis is less than that from the modified ACI 318-05 equations. In addition, the predictions by the mechanism analysis for beams with closed-type wire rope units are in good agreement with test results, regardless of the value of stresses used for the calculation of energy dissipated in wire ropes.

Keywords: strengthening, continuous T-beams, wire rope, shear, mechanism analysis.

INTRODUCTION

External shear strengthening for reinforced concrete beams would be commonly classified into two groups; bonded type and unbonded type. Many effective shear strengthening procedures[1-5] by externally bonding steel plates or high strength non-metallic fiber laminates to concrete surfaces were developed. However, few drawbacks were also identified in the bonded type strengthening technique[6-7], such as debonding of external laminates from concrete surface due to interface shear stress concentration at the laminate end, and the long term behavior of the system owing to different coefficients of thermal expansion of concrete, adhesive, and non-metallic fiber laminates. As a result, unbonded type strengthening procedures[6, 8] have been recently developed. Teng et al.[8] showed that shear capacity of deep beams predamaged in shear could be restored using external prestressed steel clamping units. Kim et al.[6] carried out tests on beams strengthened with external wire rope units and proposed that shear capacity of predamaged beams strengthened with the proposed technique could be enhanced by 120 to 170% of that of original beams. In particular, those beams strengthened with unbonded type showed ductile behavior though they failed in shear. Based on their test results, Teng et al.[8] and Kim et al.[6] concluded that the externally unbonded-type shear strengthening technique for reinforced concrete beams is highly economical, and environmentally and structurally efficient.

Although reinforced concrete beams are frequently supported on several supports and have T-shaped section, very few investigations, if any, on the shear behavior of continuous T-beams were published. Even tests on beams strengthened with externally bonded laminates have focused on simply supported beams of rectangular section. Among the few tests on the two-span continuous beams strengthened with different arrangements of carbon fiber-reinforced polymer (CFRP) laminates, El-Refaie et al.[9] pointed out that a higher load capacity could be developed in continuous beams than simple ones. In addition, the flange of externally strengthened T-beams has a significant influence on the shear behavior of those beams[5, 10]. Giaccior et al.[10] showed that shear capacity of simple T-beams

increased with the increase of width of flange if the ratio of flange depth to effective depth of beams tested was above 0.25. On the other hand, T-beams strengthened with externally bonded type procedure suffer from debonding of laminates near interface between the beam flange and web as peeling off or tensile rupture of laminates would be greatly affected by the bond and anchorage conditions at the end of laminates owing to stress concentrations[5].

The present study reports the testing of reinforced concrete continuous T-beams externally strengthened with unbonded wire rope units. Ten strengthened beams and an unstrengthened control beam were tested to failure. The amount, prestressing force and type of wire rope units were selected as the main variables to explore the significance and shortcomings of the developed shear strengthening technique. In addition, a numerical analysis based on the upper bound analysis of the plasticity theory is developed to ascertain the shear capacity of continuous T-beams strengthened with wire rope units. The shear capacity of beams tested is also compared with an extended version of the ACI 318-05 provisions[11] for shear and the proposed numerical formulas.

SIGNIFICANCE OF RESEARCH

Very few experimental investigations on shear behaviour of strengthened continuous T-beams are available, though the ratio of flange depth to effective depth, and high stress concentration at the interface between flange and web would have significant influence on the shear capacity and debonding of laminates. In addition, interest in unbonded type shear strengthening procedures using steel bars or wire ropes has increased in recent years. In the present study, the practicality, significance and shortcomings of using unbonded wire rope units as shear strengthening technique for two-span T-beams are explored. Test results and mechanism analysis based on upper-bound theorem confirm that the shear capacity of beams strengthened with closed-type wire rope units would be greatly improved with the increase of the amount and prestressing force of wire ropes.

SHEAR STRENGTHENING TECHNIQUE USING WIRE ROPE UNITS

Wire ropes have many advantages such as lightweight, high-strength, and high flexibility. The shear strengthening procedure developed for T-beams in the current investigation is distinguished into two groups: closed-type and U-type, according to the configured shape of wire rope units. For the closed-type wire rope units, a wire rope unit is comprised of an I-shaped steel plate, four legs wire rope, four sets of eye-bolts and nuts, and two corner beads of the same width as the flange of the I-shaped steel plate as shown in Fig. 1 (a). The I-shaped steel plate having four holes for eye-bolt connections is installed at the top surface of flange of beams. The longitudinal distance of holes in the I-shaped steel plate is dependent on the width of web of T-beams. U-shaped wire ropes at spacing of 60 mm are coupled to the eye-bolts passing through the holes of both sides of the beam flange. On the other hand, for the U-type wire rope units, two angles are used instead of the steel plate as shown in Fig. 1 (b). These angles having two holes for stud anchors are fixed at both sides of the beam web just below the beam flange. Eye-bolts coupled to wire ropes of 60 mm spacing are connected with nuts at the top surface of angles. As a result, there is no need to create holes in the beam flange with U-type wire rope units. In both types, corner beads having 3 mm thickness are positioned at beam corners to prevent bearing failure of concrete due to high pressure exerted by the force in wire ropes.

Wire ropes are prestressed by tightening of nuts, similar to the torque control method[12] of high-strength bolts. As the prestressing tensile effect can be controlled by the externally applied torque, the relation between the externally applied torque T and tensile force N acting on a bolt can be written as below[12]:

$$T = kd_b N \tag{1}$$

where d_b = bolt diameter and k = a torque coefficient. Many tests to evaluate the torque and tensile force relationship[6] show that the torque coefficient k of the eye-bolts employed in the wire rope units can be reasonably assumed to be 0.3.

Wire rope units would provide the beam web with a confinement effect owing to the wire rope prestressing force obtained from tightening of nuts. In addition, wire rope units would act as external stirrups to control diagonal tensile cracks and transfer shear force.

EXPERIMENTAL PROGRAMME

Test specimen details

Ten continuous beams strengthened with wire rope units and an unstrengthened control beam were tested to failure. Strengthened beams are classified into two groups: C-series and U-series for beams with closed-type and U-type wire rope units, respectively. Details of wire rope units used in test specimens are given in Table 1 and Fig. 2. In each series, the amount and prestressing force of wire rope units were varied. The ratio ρ_w of wire rope units ranged from 2.0 to 4.5 times $\rho_{\min}$, where ρ_w $= \left(= \frac{4A_{w1}}{b_w s_w} \right)$, A_{w1} = net area of single leg of wire rope, b_w = web width of beam, s_w = spacing of wire rope units, $\rho_{\min} \left(= \max\left(0.062\sqrt{f_c'}\,\frac{b_w s_w}{f_{yt}}, \frac{0.35 b_w s_w}{f_{yt}} \right) \right)$ = minimum shear reinforcement ratio specified in ACI 318-05, f_{yt} = yield strength of lateral reinforcement, which is limited to 420 MPa and f_c' = cylinder compressive strength. As a result, the spacing of wire rope units varied between 100 mm and 223 mm for C-series and between 100 mm and 178 mm for U-series. Total initial prestressing forces N_i applied in wire rope units, initial torque T_i applied in eye-bolts, the ratios between the initial prestress f_i and tensile strength f_{wu} of wire ropes for different beams tested are listed in Table 1.

All test specimens had the same section size, shear span-to-effective depth ratio a/d, longitudinal top $\rho_t \left(= \frac{A_t}{b_w d} \right)$ and bottom $\rho_b \left(= \frac{A_b}{b_w d} \right)$ reinforcement ratios, and internal shear reinforcement ratio

$\rho_v \left(= \frac{A_v}{b_w s_v} \right)$, where a = shear span, d = effective section depth, A_t and A_b = areas of longitudinal top and bottom reinforcement, respectively, and A_v and s_v = area and spacing of internal shear reinforcement, respectively. The widths of web, b_w, and flange, b_{eff}, of beams tested were 200 mm and 450 mm, respectively, and overall depths of flange, h_f, and beam section, h, were 120 mm and 400 mm, respectively. The effective depth d was 360 mm and h_f / d ratio was 0.33, for all beams tested. The shear span-to-effective depth ratio was selected to be 2.5. As a result, shear span a and length L of each span were 900 mm and 1800 mm, respectively, as shown in Fig. 2.

Both longitudinal top and bottom steel reinforcement ratios in hogging and sagging zones, respectively, were kept constant in all beams at 1.6% to ensure no flexural yielding of longitudinal reinforcement prior to shear failure. A half of longitudinal top and bottom reinforcement was anchored in the outside of the exterior supports by 90° hook and the rest of them was cut off at a distance d from points of inflection. The internal shear reinforcement of 6 mm diameter was arranged over the full length of the beams tested at 180mm spacing to satisfy the maximum spacing specified in ACI 318-05 of $d/2$. All beam flanges were transversely reinforced near the top surface across the full width of the flange with lateral steel reinforcement of 6 mm diameter at every 200mm centers, as shown in Fig. 2.

The beam notation given in Table 1 includes three parts except for the unstrengthened control beam, N. The first part is used to identify the type of wire rope units: C and U for closed and U-type wire rope units, respectively. The second part refers to $\rho_w / \rho_{\min}$ as a representative of the amount of wire rope units. The third part gives the ratio of the initial prestress in wire ropes to their tensile strength. For example, C2.5-0.6 identifies a continuous T-beam strengthened with closed-typed wire rope units having an amount of $2.5\,\rho_{\min}$ and an initial prestress of $0.6\,f_{wu}$.

Material properties

The concrete compressive strength of test specimens was designed to be as low as 24 MPa to simulate existing deteriorated concrete buildings. The ingredients of ready-mixed concrete were ordinary Portland cement, irregular gravel of maximum size of 25 mm and sand. Quality control cylinders of 150 mm diameter × 300 mm high were cast and cured simultaneously with beams to determine the compressive strength of concrete. The results of concrete compressive strength obtained from testing three cylinders for each beam are given in Table 1.

Fig. 3 and Table 2 present the stress-strain relationships and mechanical properties of internal reinforcement, wire rope, steel plate, and eye-bolt used in the present study. The wire rope used consists of six strands laid helically over a smaller independent wire rope central core. The yield strengths of 6 mm diameter reinforcement and eye-bolt were obtained from the 0.2% offset method as they did not exhibit a clear yield plateau. The elastic modulus of wire ropes used was lower than that of other metallic materials as shown in Fig. 3. Raoof and Kraincanic[13] also showed that the measured elastic modulus of wire ropes was about 60% of that of steel.

Test procedure

Loading and instrumentation arrangements are shown in Fig. 4. All beams having two spans were tested to failure under a symmetrical two-point top loading system with a displacement rate of 0.3 mm/min using a 3000 kN capacity universal testing machine (U.T.M.). Each span was identified as N-span or S-span as shown in Fig. 4. In order to evaluate the shear force at different locations and support reactions, two load cells of a 1000 kN capacity and a load cell of 2000 kN capacity were installed in both exterior end supports and intermediate support, respectively. At the location of loading or support point, steel plates of 50 mm, 75 mm, or 100 mm wide were provided to prevent premature crushing or bearing failure as shown in Fig. 4. Top loading plates were 50 mm thick and 450 mm long to cover the full flange width of test specimens.

Vertical deflections at a distance of $0.45L$ from the exterior support, which is the location of the maximum deflection predicted by a linear finite element (FE) analysis, and at the mid-span of each span were measured using linear variable differential transformers (LVDTs). Both surfaces of the beams tested were whitewashed to aid on the observation of crack development during testing. Extensor meters of 50 mm gage length were also attached to wire ropes as shown in Fig. 4 to evaluate shear transfer capacity of wire ropes, and removed after beams reached their ultimate load capacity. The tests were terminated when either a wire rope was fractured or the load dropped below 70% of the ultimate load. The test data were captured by a data logger and automatically stored.

TEST RESULTS AND DISCUSSIONS

Crack propagation, load capacity and modes of failure

The crack propagation of beams tested was strongly influenced by the type of wire rope units but nearly independent on their amount. Typical crack propagation for beams tested at different load levels is shown in Fig. 5: Fig. 5 (a) for unstrengthened control beam (N), Fig. 5 (b) for beam C2.5-0.6 as a representative specimen for beams strengthened with closed-type wire rope units, and Fig. 5 (c) for U2.5-0.6 beam as a representative specimen for beams strengthened with U-type wire rope units. Initial cracking load and the corresponding shear force are also given in Table 3. The first flexural crack generally occurred at the top surface of flange over the intermediate support, and then a flexural crack in the sagging zone immediately followed. The initial flexural cracking loads P_{fl} were little influenced by the amount and the prestressing force of wire rope units as given in Table 3. As the load increased, more flexural cracks formed and a couple of diagonal cracks developed at mid-depth of the beam web within the interior shear spans. The diagonal cracks within the interior shear spans of beams in U-series crossed the holes for stud anchors attached to the beam web.

Load capacity and the corresponding shear force at failed span of beams tested are presented in Table 3. Beams strengthened with closed type wire ropes exhibited higher load and shear capacities

than those having the same amount of U-type wire ropes. The ultimate moments recorded in both hogging and sagging regions of all beams tested were lower than the nominal moment capacity calculated from ACI 318-05 as given in Table 3. This confirms that all beams failed in shear and redistribution of internal stresses owing to yielding of longitudinal reinforcement could be ignored. The failure planes in all beams tested developed along the main diagonal crack propagated from the edge of loading plate to the bottom of beams within the interior shear span as shown in Fig. (5). In the unstrengthened beam, bond splitting crack along the longitudinal bottom reinforcement also developed together with the main diagonal crack at failure as shown in Fig. 5 (a). Other severe damage was also observed in U-series beams at the intersection of the diagonal failure plane and stud anchor holes, as shown in Fig. 5 (c). All beams exhibited the same mode of failure where two blocks formed due to the significant diagonal crack within the interior shear span. An end block rotated about the exterior support leaving the other block fixed over the other two supports as shown in Fig. 5. However, all beams were unsymmetrically failed; both S and N spans of beams tested showed nearly the same crack patterns throughout the test.

Load versus mid-span deflection

The measured beam deflection at mid-span was slightly less than that measured at $0.45L$ from the exterior support until the occurrence of the first diagonal crack within the interior shear span as predicted by the linear two-dimensional finite element (2-D FE) analysis[14]. However, the mid-span deflection was higher after the occurrence of the first diagonal crack. Therefore, the mid-span deflection of the failed span for different beams tested is only presented in Fig. 6 against the total applied load: Fig. 6 (a) for beams in C-series and Fig. 6 (b) for beams in U-series. On the same figures, mid-span deflection of the unstrengthened control beam is also given. The initial stiffness of beams tested seemed to be independent of the type, amount and prestressing force of wire rope units. The development of flexural cracks in sagging and hogging zones has little influence on the stiffness of beams tested. However, the occurrence of diagonal cracks in the interior shear span caused a

sharp decrease to the beam stiffness and increase of the beam deflection. This stiffness reduction in C-series beams was significantly influenced by the amount and prestressing force of wire rope units, indicating that the more the amount of wire rope units and the higher the prestress in wire ropes, the lower the stiffness reduction. On the other hand, the variation of stiffness after the development of the first diagonal crack in U-series beams was nearly independent on the amount of wire rope units and the prestress applied to wire ropes as the anchorage capacity of stud anchors sharply dropped after the diagonal crack passed through the stud anchor connection.

The diagonal cracking shear capacity of strengthened beams increased with the increase of the amount and initial prestressing force of wire rope units, regardless of the type of wire rope units, as given in Table 3. The ultimate shear capacity of beams strengthened with closed-type wire rope units also increased with the increase of the amount and prestressing force of wire rope units. On the other hand, the ratio of the ultimate shear capacity of beams strengthened with U-type wire rope units to that of the control unstrengthened beam ranged only between 1.05 and 1.14, revealing that the shear capacity of those beams was little influenced by the amount and prestressing force of wire rope units. After the occurrence of the main diagonal crack, anchorage failure of stud anchor in beams with U-type wire rope units would fail to provide concrete with an effective confinement and the amount of shear force transferred by truss action of wire ropes would be very small.

The influence of the amount and prestressing force of wire ropes on the load-deflection relationship after the ultimate load capacity was greatly dependent on the type of wire rope units. All beams in C-series except C2-0.6 and C2.5-0.75 specimens showed a ductile failure in spite of failing in shear, and fracture of wire ropes of these beams occurred at large defection. For C2.5-0.75 specimen, sooner after it reached its ultimate load capacity, wire ropes started to rupture. On the other hand, the mode of failure of beams in U-series was more brittle than that of unstrengthened beam due to anchorage failure of stud anchors connected to the beam web. It can be concluded that closed-type

wire rope units having a larger amount than 2.5 $\rho_{\min}$ and an initial prestress below 0.6 f_{wu} would be an optimum arrangement to improve the shear capacity and ductility of reinforced concrete T-beams.

Stresses in wire ropes

Fig. 7 shows the amount of stresses developed in wire ropes against the total applied load. The upper stress limits for design of shear reinforcement specified in ACI 318-05 is also presented in the same figure. Stresses developed in wire ropes presented in Fig. 7 were calculated as below. Strains in wire ropes were first estimated as the ratio of average displacement measured using the extensor meter attached to wire ropes crossing the diagonal crack within the interior shear span to the gage length of 50 mm. Initial strains due to initial prestress were offset from the measured strains at different stages of loading. These strains were finally converted into corresponding stresses using the stress-strain curve of wire ropes shown in Fig. 3. The stresses in wire ropes sharply increased with the occurrence of the first diagonal crack, regardless of the type, amount and initial prestressing force of wire rope units. The stresses developed in wire ropes at ultimate strength of C-series beams ranged between 390 MPa and 510 MPa. On the other hand, for U-series beams, stresses developed in wire ropes at beam ultimate strength were below 260 MPa, indicating that wire rope units could not effectively contribute to load transfer due to the anchorage failure of stud anchors used to fix wire rope units.

PREDICTION OF SHEAR CAPACITY USING ACI 318-05

The empirical equations specified in ACI 318-05 for estimating shear capacity V_n for reinforced concrete elements can be extended to accommodate the effect of external wire rope units considered for the beams tested as follows:

$$V_n = V_c + V_s + V_w \tag{2}$$

where $V_c \left[= \left(0.16\sqrt{f_c^{'}} + 17\rho_t \frac{V_u d}{M_u} \right) b_w d \le 0.29\sqrt{f_c^{'}} b_w d \right]$ = shear capacity of concrete, V_s = shear transfer capacity of internal shear reinforcement, and V_w = shear transfer capacity of wire ropes, V_u = factored shear force, M_u = factored moment occurring simultaneously with V_u at section considered, and ρ_t = longitudinal tensile reinforcement ratio. As shear transfer mechanism of lateral reinforcement is identified by 45° truss analogy, the shear transfer capacities of internal shear reinforcement and external wire ropes can be assumed as below:

$$V_s + V_w = A_v f_{yh} d / s_v + A_w f_{ws} d / s_w \tag{3}$$

where A_v , f_{yh} and s_v = area, yield strength, and spacing of internal shear reinforcement, respectively, f_{ws} = stress developed in wire ropes at beam ultimate strength. In shear provisions of ACI 318-05, the shear transfer capacity and yield strength of lateral reinforcement are limited to be below $0.66\sqrt{f_c^{'}} b_w d$ and 420 MPa, respectively, to control diagonal crack width and induce ductile failure by yielding of shear reinforcement. If stresses f_{ws} in wire ropes are not measured, a notional stress f_{ws} of wire ropes would be assumed as follows:

$$f_{ws} = f_{wu} - f_i \le 420\,\text{MPa} \tag{4}$$

Comparisons of shear capacities obtained from experiments and Eqs. (2) and (3) developed from ACI 318-05 are presented later in this paper.

MECHANISM ANALYSIS OF BEAMS TESTED

All beams tested in the current study failed due to diagonal shear cracks as shown in Fig. 5; however, this failure was ductile, especially for beams with external closed wire ropes. Fig. 8 presents an idealization of the unsymmetrical failure mode of two-span T beams strengthened with wire rope units. As proposed by Zhang[18], a yield line can generally be represented as a parabolic line connecting the edges of the loading plate and a point at a finite distance from the intermediate

support. As a result, continuous beams, at collapse, usually can be idealized as an assemblage of two rigid blocks separated by a yield line. The rigid block *II* is fixed over the intermediate and exterior supports and the other rigid block *I* rotates about an instantaneous centre (I.C.) as experimentally observed at the beam failure.

Modeling of materials

Concrete is modelled as a rigid perfectly plastic material obeying the modified Coulomb failure criteria with zero tension cutoff[19]. The effective compressive strength, f_c^*, to be used in calculation is obtained from the cylinder compressive strength , $f_c^{'}$, as follows:

$$f_c^* = \xi \nu_e f_c^{'} \tag{5}$$

where ν_e = effectiveness factor for cracked concrete, and ξ = strength enhancement factor of concrete under biaxial compressive stresses.

Tensile and compressive reinforcement are generally assumed as a rigid perfectly plastic material with yield stress f_y. However, Yang et al.[20] pointed out that the value of f_y of longitudinal reinforcement would need to be limited to 420 MPa, as high-strength longitudinal reinforcement may not reach its yield strength, if the amount of reinforcement is heavy and failure in concrete is preceded. On the other hand, the potential stress development in wire ropes at the ultimate strength of strengthened beams can be idealized to be the difference between the tensile strength of wire ropes and initial prestress in wire ropes, $f_{wu} - f_i$. Considering test results of stress development in wire ropes and the upper limit specified in ACI 318-05, a nominal stress in wire ropes can be assumed similar to that given in Eq. (4). In this study, therefore, nominal values for stresses in internal shear reinforcement and external wire ropes are limited to 420 MPa when no actual stresses measured from tests are provided.

Effectiveness factor of cracked concrete

Although concrete is a typical brittle material, it is regarded as a perfectly plastic material in the plasticity theory. To absorb this gap and other shortcomings of applying the theory of plasticity to concrete, an effectiveness factor ν_e for cracked concrete would be commonly introduced. From the crack sliding solution for short beams, Zhang[18] proposed the following formula for ν_e:

$$\nu_e = \nu_o \nu_s \tag{6}$$

where ν_s = the sliding resistance reduction factor, which is suggested to be 0.5 by Zhang[18] when the yield line follows the crack path, and ν_o = effectiveness factor for uncracked concrete. Based on the test results on short beams, ν_o was proposed as below[18]:

$$\nu_o = \frac{0.548}{\sqrt{f_c'}}\left(1+\frac{1}{\sqrt{h}}\right)(0.259\rho_t + 1) \tag{7}$$

where h = overall section depth in m.

Strength enhancement factor of concrete

The compressive strength enhancement of concrete under biaxial stresses is mainly dependent on the biaxial stress ratio. Kupfer et al.[15] showed that the strength of concrete under biaxial compressive stresses was up to 27% higher than the uniaxial compressive strength of concrete. However, the strength of concrete subjected to biaxial tensile stresses was approximately equal to uniaxial tensile strength[15]. Liu et al.[16] proposed an empirical formula and a failure envelope to evaluate biaxial strength of concrete, and pointed out that the maximum increasing ratio of concrete strength was close to 20% when the biaxial stress ratio was 0.2. A strength increase of about 31% for normal strength concrete under biaxial compressive stresses was also observed in Hussein and Marzouk's experiments[17].

The compressive strength of concrete confined by wire rope units would be higher than that obtained from uniaxial cylinder tests, as the prestress in wire ropes allows confined concrete to be in a state of

biaxial stresses. However, it is very difficult to ascertain the biaxial stress ratio in the confined concrete of the strengthened beams at this stage. Based on tests of reinforced concrete beams confined with unbonded closed type wire rope units, Kim et al.[6] studied the concrete confinement owing to unbonded closed type wire ropes and concluded that strength enhancement factor ξ is linearly increased with the vertical stress $f_{vi}\left(\approx 0.9\frac{N_i}{b_w s_w}\right)$ in wire ropes. Therefore, the strength enhancement factor ξ for concrete confined by closed-type wire rope units is simply assumed as $\xi = 1.0 + 0.0334 f_{vi}$. As U-type wire rope units would seldom provide the concrete webs with an effective confinement due to anchorage failure of stud anchors, the strength of concrete confined with U-type wire rope units can be regarded as that of unconfined concrete under uniaxial stress (ξ = 1.0).

Work Equation

The upper-bound theorem is based on the energy principle, by equating the total internal energy, W_I, to the external work, W_E. The total internal energy mainly depends on the position of the instantaneous center and the amount of internal stresses in both concrete along the yield line and reinforcement crossing the yield line. As the relative displacement rate δ equals $\omega \cdot r$ as shown in Fig. 8(a), the energy, W_c, dissipated in concrete in the hyperbolic yield line proposed by Nielsen[19] can be modified as follows:

$$W_c = \frac{b_w f_c^*}{2}\omega r_w(1-\sin\alpha_w)\frac{h}{\sin\beta} + \frac{(b_{eff}-b_w) f_c^*}{2}\omega r_f(1-\sin\alpha_f)\frac{h_f}{\sin\beta} \quad (8)$$

where r = distance between the midpoint of the chord of the yield line and the instantaneous center; ω = rotational displacement of rigid block *I*; α = angle between the relative displacement at the midpoint of the chord and yield line chord; and β = angle between the yield line chord and beam longitudinal axis as shown in Fig. 8(a). Subscripts f and w refer to the overhanging flange section

and the remaining rectangular beam section, respectively. From the extended crack sliding solution for beams with shear reinforcement, Hoang[21] derived a formula for the starting point x of the yield line from the edge of the support plate as a function of the amount of vertical shear reinforcement used in beams failed in shear. This proposed formula for x was subsequently verified by Cho[12] from the comparisons with test results of beams having shear span to depth ratio a/d of 2.5. It can be modified to accommodate the effect of the external wire units as below:

$$x = x_e - \left(\sqrt{0.118 v_0 /(\psi_v + \psi_w)}\right) h \tag{9}$$

where x_e = clear shear span, ψ_v (= $\rho_v f_y / f_c^{'}$)= mechanical degree of internal shear reinforcement, and ψ_w (= $\rho_w f_{ws} / f_c^{'}$)= mechanical degree of wire ropes used as external shear reinforcement. Therefore, β can be calculated from $\tan^{-1}\left[h/(x_e - x)\right]$ as shown in Fig. 8(a).

The relative displacement of internal reinforcement δ_s can be expressed as $\omega \cdot r_s$ as shown in Fig. 8(b). Therefore, the energy W_s dissipated in steel reinforcement crossing the yield line is:

$$W_s = \sum_{i=1}^{n} \omega (A_s)_i (f_y)_i (r_s)_i \cos(\alpha_s)_i \tag{10}$$

where n = the number of reinforcing bars crossing the yield line, $(A_s)_i$, and $(f_y)_i$ = area and yield strength of the reinforcing bar i crossing the yield line, respectively, $(r_s)_i$ = distance between the reinforcing bar i and the instantaneous centre, and $(\alpha_s)_i$ = angle between the relative displacement δ_s about I.C. and the reinforcing bar i crossing the yield line (see Fig. 8(b)). The relative displacement of wire ropes δ_r can be also expressed as $\omega \cdot r_r$; hence, the energy W_w dissipated in wire rope crossing the yield line can be similarly calculated from:

$$W_w = \sum_{j=1}^{m} \omega (A_w)_j (f_{ws})_j (r_r)_j \cos(\alpha_r)_j \tag{11}$$

where m = the number of wire ropes crossing the yield line, $(A_w)_j$, and $(f_{ws})_j$ = area and stress of the wire rope j crossing the yield line, respectively, $(r_r)_j$ = distance between the wire rope j and the instantaneous center, and $(\alpha_r)_j$ = angle between the relative displacement δ_r about I.C. and the wire rope j crossing the yield line as shown in Fig. 8(b).

The external work W_E done by the vertical load $P_n/2$ on rigid block *I* shown in Fig. 8(a) can be expressed as follows:

$$W_E = \frac{P_n}{2}\omega a \tag{12}$$

Equating the total internal energy dissipated in concrete, internal reinforcement and wire ropes to the external work done, the load capacity P_n can be written in the following form:

$$P_n = \frac{b_w h}{a}\left[\begin{array}{l} f_c^{\,*} r_w(1-\sin\alpha_w)\dfrac{1}{\sin\beta} + (b_{eff}/b_w - 1) f_c^{\,*} r_f (1-\sin\alpha_f)\dfrac{h_f}{h\sin\beta} \\ + 2\sum_{i=1}^{n}(\rho_s)_i (f_y)_i (r_s)_i \cos(\alpha_s)_i + 2\sum_{j=1}^{m}(\rho_w)_j (f_{ws})_j (r_r)_j \cos(\alpha_r)_j \end{array}\right] \tag{13}$$

where $(\rho_s)_i \left[=(A_s)_i / b_w h\right]$= the ratio of reinforcement i crossing the yield line to the section area, and $(\rho_w)_j \left[=(A_w)_j / b_w h\right]$= the ratio of wire rope j crossing the yield line to the section area.

Elastic analysis of two-span continuous beams shows that the shear force V_n within the interior shear span can be expressed as $0.344P_n$. However, current test results clearly showed that an average value of the measured V_n/P_n ratio was around 0.306 as given in Table 3 as the occurrence of diagonal cracks within interior shear spans decreased the load transferred to the intermediate support, regardless of the type of wire rope units. Therefore, the ultimate shear capacity of continuous T-beams can be obtained from the load capacity predicted by the proposed mechanism analysis using the relation of $V_n = 0.306P_n$.

Solution procedure

The beam load capacity is implicitly expressed as a function of the position of the instantaneous center (X_{ic}, Y_{ic}) as given in Eq. (13). The horizontal coordinate X_{ic} of the instantaneous center coincide with that of the global coordinates at the exterior support as the vertical displacement of rigid block *I* is prevented at the exterior support as shown in Fig. 8. According to the upper-bound theorem, the collapse occurs at the minimum resistance. The minimum value of capacity is determined by varying the vertical coordinate Y_{ic} of the instantaneous center along the vertical axis of the global coordinate. The process of tuning the vertical coordinate Y_{ic} to get the minimum value of the load capacity is achieved by reliable numerical optimization procedures provided in Matlab software[23].

COMPARISONS OF TEST RESULTS AND PREDICTIONS

Comparisons between the predictions obtained from the modified equations based on ACI 318-05 or the proposed numerical formulas and experimental results of the ultimate shear capacity V_n of beams strengthened with wire rope units are given in Table 4. The shear transfer capacity of wire rope units is calculated using either the actual stresses in wire ropes crossing the failure plane measured from experiments or the notional stresses of wire ropes given by Eq. (4). When the notional stresses of wire ropes are employed, the predictions obtained from the modified equations of ACI 318-05 are unconservative for beams U3.5-0.6 and U4.5-0.6. On the other hand, all beams tested are conservatively predicted by the modified equations of ACI 318-05 using the actual stresses of wire ropes measured from experiments, with an average and standard deviation of the ratios between the experimental and theoretical shear capacities of beams tested of 1.37 and 0.15, respectively. For the mechanism analysis of the U-series beams, the ratios between measured and predicted shear capacities are much lower when notional stresses of wire ropes are employed than measured stresses. A smaller coefficient of variation is achieved in case of the mechanism analysis

than ACI 318-05 as shown in Table 4. When the stresses measured in wire ropes are used, load and shear capacities obtained from the mechanism analysis are in better agreement with experimental results. In particular, for beams strengthened with closed-type wire rope units, the predictions by the mechanism analysis show good agreement with test results, regardless of the actual or notional stress of wire ropes, employed for the calculation of energy dissipated in wire ropes.

CONCLUSIONS

Ten reinforced concrete continuous T-beams externally strengthened with wire rope units and an unstrengthened control beam were tested to failure. Closed type wire ropes were more effective than U-type wire ropes in enhancing beam capacity and ductility. Mechanism analysis based on the upper bound analysis of the plasticity theory are developed to evaluate the ultimate shear capacity of beams tested. The following conclusions may be drawn:

1. The failure plane of two-span continuous T-beams was formed unsymmetrically within one interior shear span only, along a diagonal crack connecting the edge of the loading plate and a point at a finite distance from the intermediate support.
2. After the occurrence of the first diagonal crack, the increasing rate of deflection of beams with closed-type wire rope units decreased with the increase of the amount and prestressing force of wire rope units, whereas the stiffness reduction of beams with U-type wire rope units was nearly independent on the amount and prestress in wire rope units.
3. The ultimate shear capacity of beams strengthened with closed-type wire rope units increased with the increase of the amount and prestressing force of wire rope units, while that of beams with U-type wire rope units was little influenced by the amount and prestressing force of wire rope units.
4. When the amount of wire ropes was above 2.5 times the minimum amount of shear reinforcement specified in ACI 318-05 and the prestress applied in wire ropes was less than

60% of its tensile strength, beams with closed-type wire rope units failed in a ductile mode. However, the mode of failure of beams with U-type wire rope units was more brittle than that of the unstrengthened control beam due to anchorage failure of stud anchors.

5. The measured intermediate support reaction at the ultimate strength of beams tested was lower than predictions obtained from a two-dimensional linear finite element analysis by an average of 11%. The redistribution of applied load after the first diagonal crack was hardly influenced by the type, amount, and prestressing force of wire rope units.
6. The average stresses developed in wire ropes at ultimate strength of beams tested with closed-type wire rope units ranged between 390 MPa and 510 MPa, whereas, those of beams with U-type wire rope units were below 260 MPa.
7. The modified equations based on the ACI 318-05 provisions for shear are unconservative for beams with U-type wire rope units when notional stresses of wire ropes are employed, but conservative for all beams tested when the average actual stresses of wire ropes measured from experiments are used.
8. The load and shear capacities obtained from the mechanism analysis are in better agreement with experimental results when the average actual stresses of wire ropes are employed.

ACKNOWLEDGMENT

This work was supported by the Regional Research Center Program (BIO-housing Research Institute), granted by the Korean Ministry of Education & Human Resources Development.

REFERENCES

1. ACI Committee 440, State-of-the-Art Report on Fiber-Reinforced Plastic (FRP) Reinforcement for Concrete Structures (ACI 440R-96), American Concrete Institute, Farmington Hills, MI, 1996, 65 pp.

2. Islam, M. R., Mansur, M. A., and Maalej, M., "Shear Strengthening of RC Deep Beams using Externally Bonded FRP systems," Cement & Concrete Composites, V. 27, 2005, pp. 413-420.
3. Vilnay, O., "The analysis of Reinforced Concrete Beams Strengthened by Epoxy-Bonded Steel Plates," The International Journal of Cement Composites and Lightweight Concrete, V.10, No. 2, 1988, pp. 73-78.
4. Malek, M., and Saadatmanesh, H., "Ultimate Shear Capacity of Reinforced Concrete Beams Strengthened with Web-Bonded Fiber-Reinforced Plastic Plates," ACI Structural Journal, V. 95, No. 4, 1998, pp. 391-399.
5. Triantafillou, T. C., "Shear Strengthening of Reinforced Concrete Beams using Epoxy-Bonded FRP Composites," ACI Structural Journal, V. 95, No. 2, 1998, pp. 107-115.
6. Kim, S. Y., Yang, K. H., Byun, H. Y., and Ashour, A. F., "Tests of Reinforced Concrete Beams Strengthened with Wire Rope Units," Engineering Structures, doi:10.1016/j.engstruct. 2006.12.013, 2007.
7. Oehlers, D. J., and Moran, J. P., "Premature Failure of Externally Plated Reinforced Concrete Beams," Journal of Structural Engineering, ASCE, V. 116, No. 4, 1990, pp. 978-993.
8. Teng, S., Kong, F. K., Poh, S. P., Guan, L. W., and Tan, K. H., "Performance of Strengthened Concrete Deep Beams Predamaged in Shear," ACI Structural Journal, V. 93, No. 2, 1996, pp. 159-171.
9. El-Refaie, S. A., Ashour, A. F., and Garrity, S. W., "Sagging and Hogging Strengthening of Continuous Reinforced Concrete Beams Using Carbon Fiber-Reinforced Polymer Sheets," ACI Structural Journal, V. 100, No. 4, 2003, pp. 446-453.
10. Giaccio, C., Al-Mahaidi, R., and Taplin, G., "Experimental Study on the Effect of Flange Geometry on the Shear Strength of Reinforced Concrete T-Beams subjected to Concentrated Loads," Canadian Journal of Civil Engineering, V. 29, No. 6, 2002, pp. 911-918.

11. ACI Committee 318: Building Code Requirements for Structural Concrete (ACI 318-05) and Commentary (ACI 318R-05). American Concrete Institute, 2005. 436 pp.

12. Bickford, J. H., An Introduction to the Design and Behavior of Bolt Joints, Marcel Dekker INC. 1990.

13. Raoof, M., and Kraincanic, I., "Analysis of Large Diameter Steel Ropes," Journal of Engineering Mechanics, ASCE, V. 121, No. 6, 1995, pp. 667-675.

14. Červenka, V., and Červenka, J., ATENA Computer Program for Non-Linear FEM Analysis of Reinforced Concrete Structures, Cervenka Consultant, 2003.

15. Kupfer, H., Hilsdorf, H. K., and Rusch, H., "Behavior of Concrete Under Biaxial Stresses," ACI Journal, Proceedings, V. 66, No. 8, 1969, pp. 656-666.

16. Liu, T. C. Y., Nilson, A. H., and Slate, F. O., "Stress-Strain Response and Fracture of Concrete in Uniaxial and Biaxial Compression," ACI Journal, Proceedings, V. 69, No. 3, 1972, pp. 291-295.

17. Hussein, A., and Marzouk, H., "Behavior of High-Strength Concrete under Biaxial Stresses," ACI Materials Journal, V. 97, No. 1, 2000, pp. 27-36.

18. Zhang, J. P., "Diagonal Cracking and Shear Strength of Reinforced Concrete Beams," Magazine of Concrete Research, V. 49, No. 178, 1997, pp. 55-65.

19. Nielsen M. P. *Limit Analysis and Concrete Plasticity*, Prentice-Hall, Englewood Cliffs, 1984.

20. Yang, K. H., Chung, H. S., and Ashour, A. F., "Influence of Section Depth on the Structural Behavior of Reinforced Concrete Continuous Deep Beams," Magazine of Concrete Research, V. 59, doi:10.1680/macr.2007.59.001.

21. Hoang, L. C., "Shear Strength of Lightly Shear Reinforced Concrete Beams," Series R, No. 65, Dept. of Structural Engineering and Materials, Technical University of Denmark, 2000, 172 pp.

22. Cho, S. H., "Shear Strength Prediction by Modified Plasticity Theory for Short Beams," ACI Structural Journal, V. 100, No. 1, 2003, pp. 105-112.

23. Chapman, S. J., MATLAB Programming for Engineers, Thomson, USA, 2004.

Table 1–Details of test specimens

Specimen	f_c' MPa	Details of wire rope unit						
		Type	ρ_w	$\frac{\rho_w}{\rho_{\min}}$	s_w mm	f_i / f_{wu}	N_i kN	T_i N·m
N	26.8	N/A						
C2.0-0.6	25.9	Closed Type	0.0017	2.0	223	0.6	78.8	37.5
C2.5-0.6	25.9		0.0021	2.5	178			
C3.5-0.6	26.4		0.0029	3.0	127			
C4.5-0.6	26.4		0.0038	4.5	100			
C2.5-0.45	25.0		0.0021	2.5	178	0.45	59.1	28.1
C2.5-0.75	26.4		0.0021	2.5	178	0.75	98.5	47.5
U2.5-0.6	26.7	U type	0.0021	2.5	178	0.6	78.8	37.5
U3.5-0.6	26.7		0.0029	3.5	127			
U4.5-0.6	26.7		0.0038	4.5	100			
U2.5-0.75	26.7		0.0021	2.5	178	0.75	98.5	47.5

Note : f_c' = cylinder compressive strength, ρ_w = ratio of wire rope unit $\left(=\frac{4A_{w1}}{b_w s_w}\right)$, A_{w1} = net area of single leg of wire rope, b_w = web width of beam, s_w = spacing of wire rope units, $\rho_{\min}\left(=\max\left(0.062\sqrt{f_c'}\frac{b_w s_w}{f_{yt}}, \frac{0.35 b_w s_w}{f_{yt}}\right)\right)$ = minimum shear reinforcement ratio specified in ACI 318-05, f_{yt} = yield strength of lateral reinforcement, which is limited to 420 MPa, f_i = prestress applied in wire rope, f_{wu} = tensile strength of wire rope, N_i = total prestressing force of a wire rope unit, and T_i = initial torque applied to eye-bolt.

Table 2–Mechanical properties of metallic materials

Type	Dia., mm	A_{net}, mm^2	f_y, MPa	ε_y	f_u, MPa	E_s, GPa
Reinforcement	19	287	486	0.003	665	202.9
	6	28.3	388*	0.0037	433	205.8
Steel plate	-	600	269.9	0.00138	353	195.5
Eye-bolt	13	119.3	492*	0.0044	706	205.3
Wire rope	6.3	18.6	-	-	1765	123.5

Note : A_{net} = net area, f_y = yield strength, ε_y = yield strain, f_u = tensile strength, and E_s = elastic modulus.

* The yield strengths of 6 mm diameter reinforcement and 13 mm eye-bolt were obtained from the 0.2% offset method.

Table 3–Summary of test results

Specimen	Initial flexural cracking load P_{fl}, (kN)		Diagonal cracking load (P_{cr}) and shear force (V_{cr}), (kN)				Load capacity (P_n) and corresponding shear force (V_n) at failed span, (kN)			Ultimate moment (M_n), (kN· m)		$\frac{(M_n)_N}{(M_{fl})_N}$	$\frac{(M_n)_P}{(M_{fl})_P}$
			Interior		Exterior								
	$(P_{fl})_N$	$(P_{fl})_P$	$(P_{cr})_I$	$(V_{cr})_I$	$(P_{cr})_E$	$(V_{cr})_E$	P_n	$(V_n)_I$	$(V_n)_E$	$(M_n)_N$	$(M_n)_P$		
N	166.6	215.0	390.3	126.1	547.9	97.9	580.1	182.0	108.0	66.6	97.2	0.37	0.52
C2.0-0.6	178.2	197.2	411.5	131.6	555.9	103.3	707.2	214.9	138.5	68.9	124.7	0.39	0.67
C2.5-0.6	170.6	210.3	417.4	133.1	564.7	104.1	799.9	239.7	159.6	72.7	143.6	0.41	0.77
C3.5-0.6	176.9	218.9	431.6	137.8	565.8	103.7	966.5	308.2	174.9	120.1	157.4	0.67	0.84
C4.5-0.6	187.7	222.5	437.6	141.3	608.2	111.2	1063.7	341.6	190.5	135.8	171.5	0.76	0.92
C2.5-0.45	160.2	212.8	424.5	130.9	564.7	104.7	756.8	218.8	160.2	52.2	144.2	0.29	0.78
C2.5-0.75	181.6	220.2	418.6	135.7	575.9	103.4	868.5	269.3	165.8	92.4	149.2	0.52	0.80
U2.5-0.6	176.8	221.9	398.2	125.8	530.0	98.8	622.8	191.0	120.9	62.6	108.8	0.35	0.58
U3.5-0.6	172.5	215.5	394.8	124.5	546.6	101.1	617.6	191.0	118.1	65.3	106.3	0.37	0.57
U4.5-0.6	185.3	226.0	411.3	130.9	532.6	100.5	647.9	193.0	130.2	57.2	117.2	0.32	0.63
U2.5-0.75	184.0	217.5	410.2	131.4	589.3	109.4	689.5	208.0	136.4	64.8	122.8	0.36	0.66

Note : M_{fl} indicates the nominal moment capacity of beam section obtained from ACI 318-05.

Subscripts N and P indicate the hogging and sagging zones, respectively.

Interior and exterior shear spans are identified by subscripts I and E, respectively.

Table 4–Comparisons of test results and predictions

Specimen	Experiments		ACI 318-05		Numerical analysis				Exp./Pre.					
									ACI 318-05		Numerical analysis			
	f_{ws} MPa	V_n kN	$(V_n)_R$ kN	$(V_n)_N$ kN	$(P_n)_R$ kN	$(P_n)_N$ kN	$(V_n)_R$ kN	$(V_n)_N$ kN	$\frac{(V_n)_{Exp.}}{(V_n)_{R\_Pre.}}$	$\frac{(V_n)_{Exp.}}{(V_n)_{N-Pre.}}$	$\frac{(P_n)_{Exp.}}{(P_n)_{R\_Pre.}}$	$\frac{(P_n)_{Exp.}}{(P_n)_{N-Pre.}}$	$\frac{(V_n)_{Exp.}}{(V_n)_{R\_Pre.}}$	$\frac{(V_n)_{Exp.}}{(V_n)_{N-Pre.}}$
N	-	182.0	112.5	112.5	605.0	605.0	185.0	185.0	1.62	1.62	0.96	0.96	0.98	0.98
C2.0-0.6	388	214.9	158.1	162.0	769.0	780.0	235.0	238.8	1.36	1.33	0.92	0.91	0.91	0.90
C2.5-0.6	478	239.7	183.5	174.8	906.0	874.0	277.0	267.6	1.31	1.37	0.88	0.92	0.87	0.90
C3.5-0.6	513	308.2	220.3	200.7	1007.1	944.9	308.8	289.1	1.40	1.54	0.96	1.02	1.00	1.07
C4.5-0.6	468	341.6	237.5	224.6	1033.7	998.0	316.3	305.4	1.44	1.52	1.03	1.07	1.08	1.12
C2.5-0.45	415	218.8	173.0	173.8	867.0	870.5	265.5	266.4	1.26	1.26	0.87	0.87	0.82	0.82
C2.5-0.75	350	269.3	164.8	175.3	839.2	878.5	256.8	268.8	1.63	1.54	1.03	0.99	1.05	1.00
U2.5-0.6	227	191.0	146.6	175.7	709.4	783.6	217.1	239.8	1.30	1.09	0.88	0.79	0.88	0.80
U3.5-0.6	167	191.0	147.7	201.1	695.6	800.1	212.8	244.8	1.29	0.95	0.89	0.77	0.90	0.78
U4.5-0.6	234	193.0	175.2	225.0	763.7	846.2	233.7	258.9	1.10	0.86	0.85	0.77	0.83	0.75
U2.5-0.75	260	208.0	151.6	175.7	722.8	783.6	221.2	239.8	1.37	1.18	0.95	0.88	0.94	0.87
Mean									1.37	1.30	0.93	0.90	0.93	0.91
Standard deviation									0.15	0.25	0.06	0.10	0.08	0.12
Coefficient of variation									0.11	0.19	0.06	0.11	0.09	0.13

Note: Subscripts R and N indicate values calculated using actual stress of wire ropes measured in the current study and the notional stress in wire ropes given by Eq. (4), respectively.

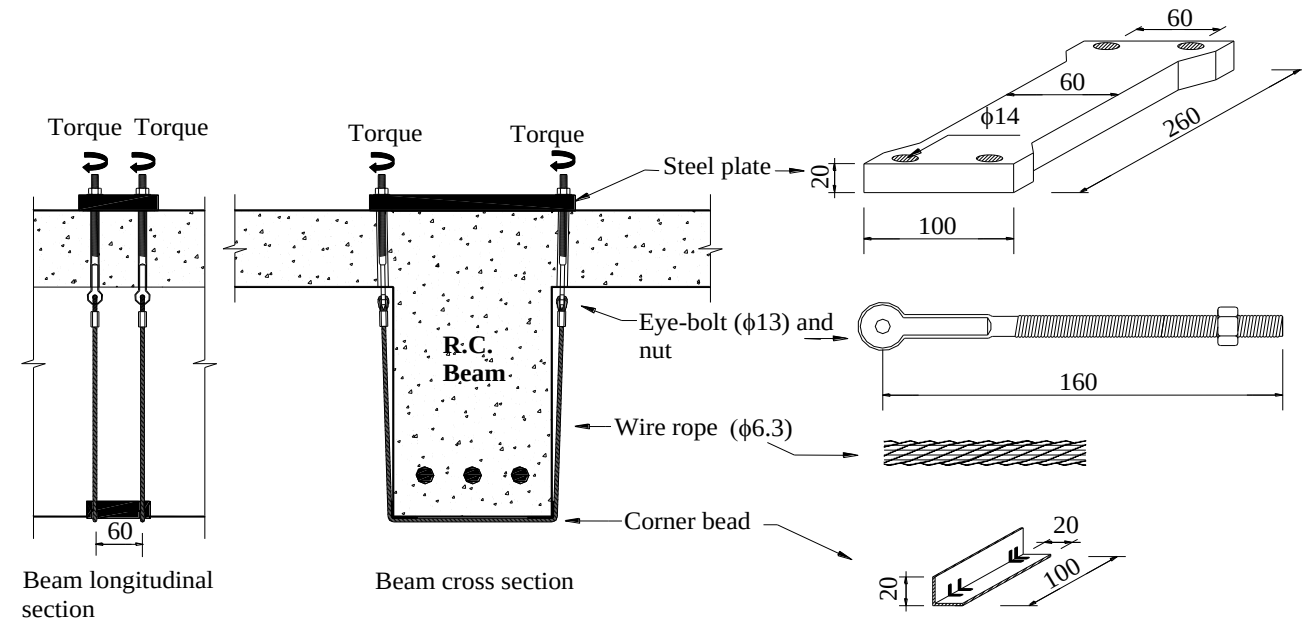

(a) Closed-type wire rope unit

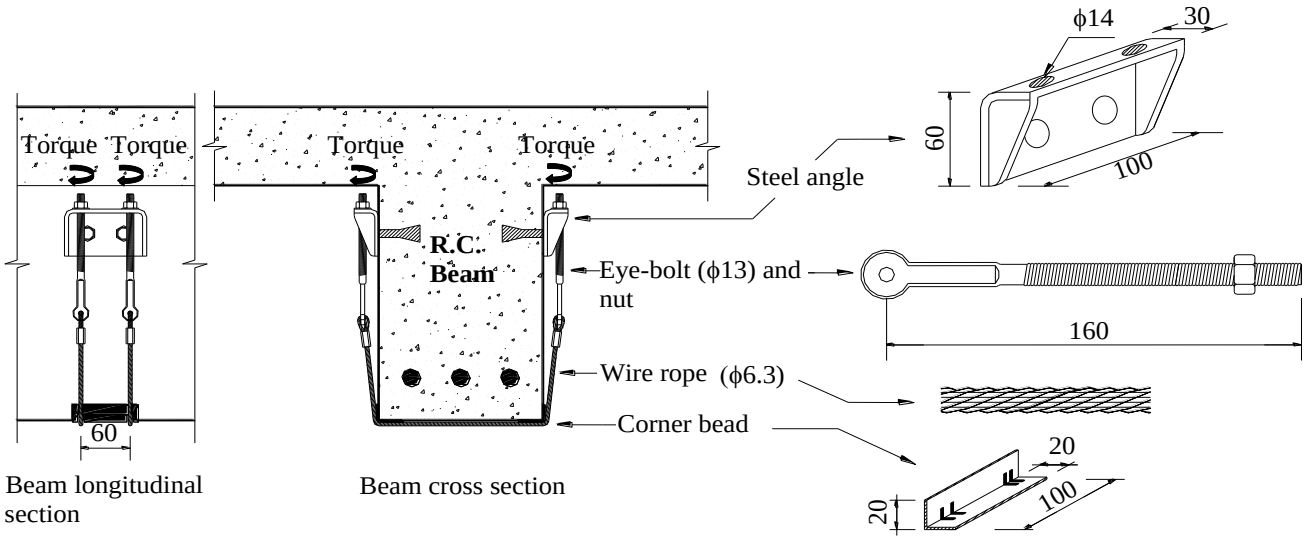

(b) U-type wire rope unit

Fig. 1-Details of developed wire rope units and strengthening procedure.

(all dimensions are in mm)

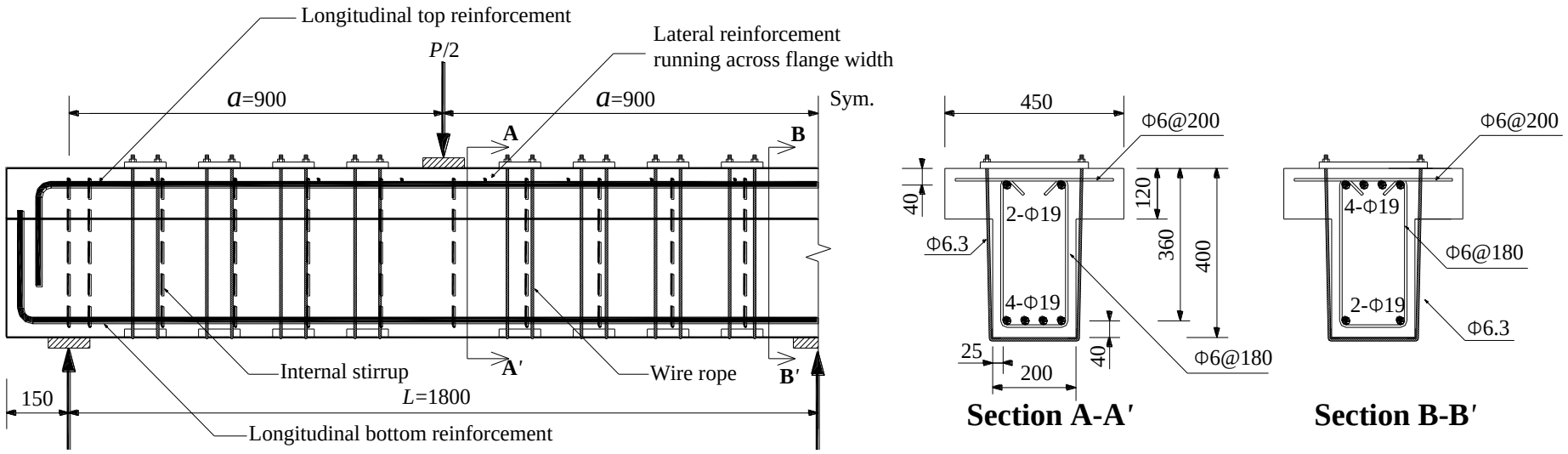

(a) Beams strengthened with C-type wire rope units

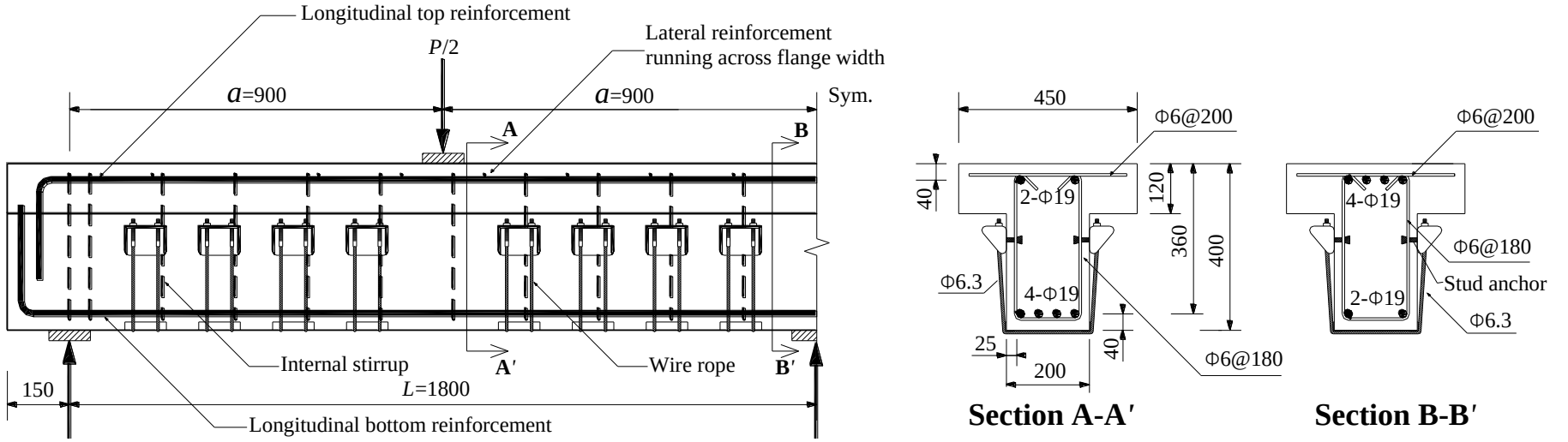

(b) Beams strengthened with U-type wire rope units

Fig. 2-Specimen details and arrangement of reinforcement and wire rope units. (all dimensions are in mm)

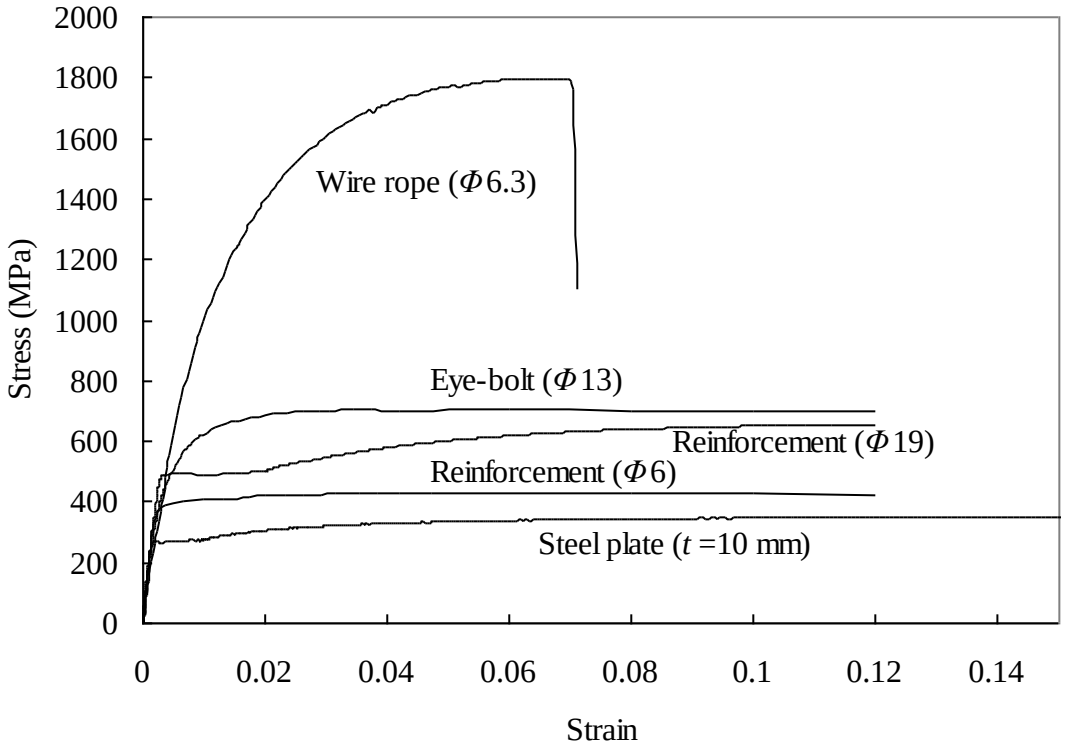

Fig. 3-Stress-strain relationships of metallic materials.

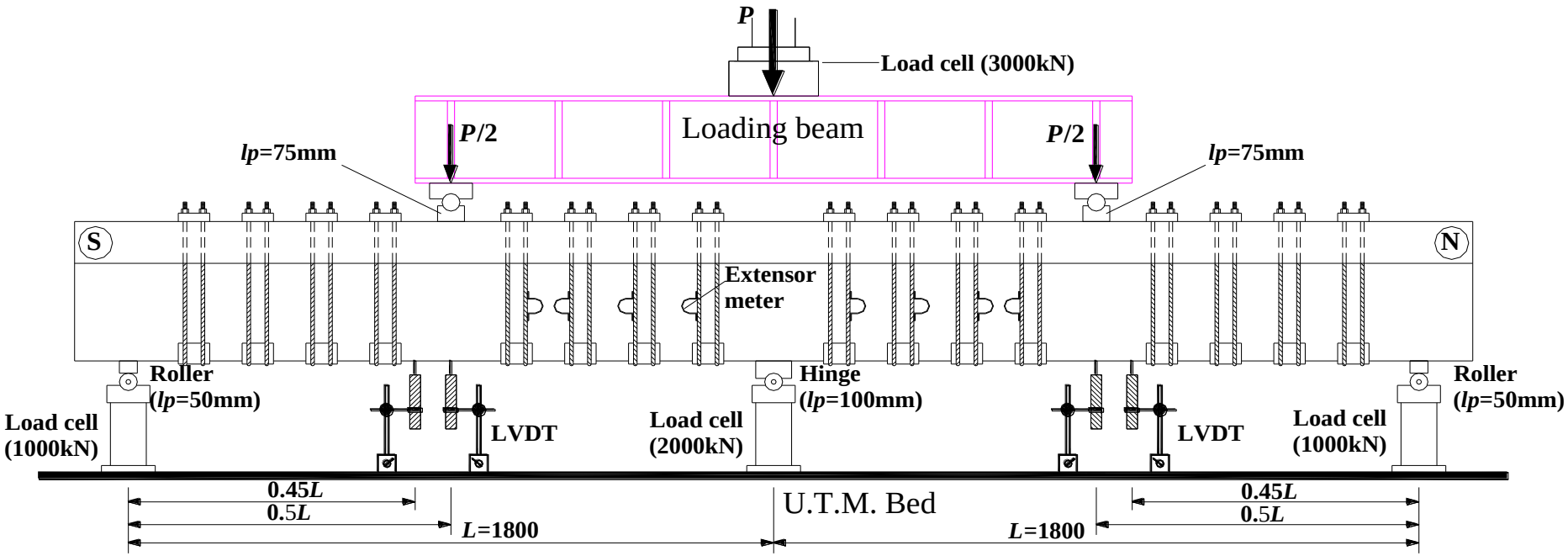

Fig. 4-Test setup (All dimensions are in mm).

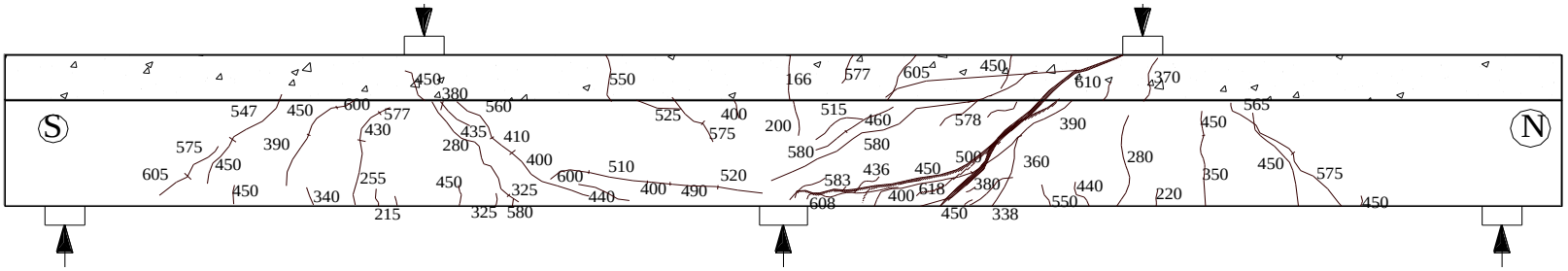

(a) N

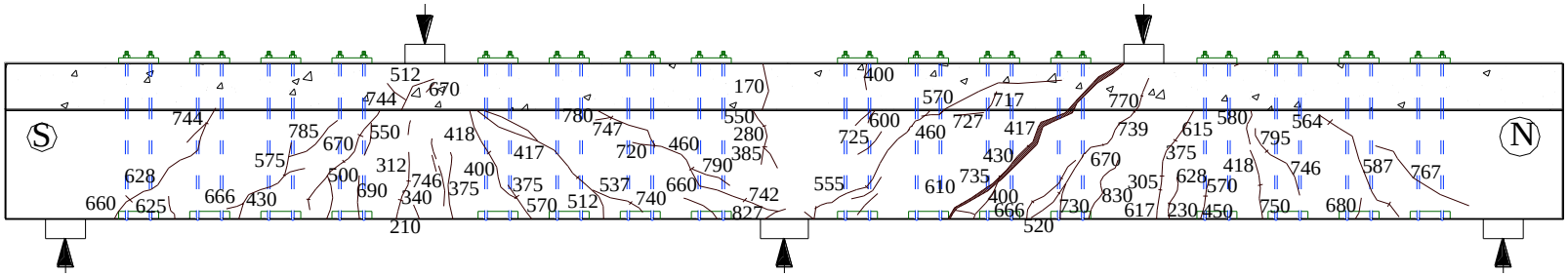

(b) C2.5-0.6

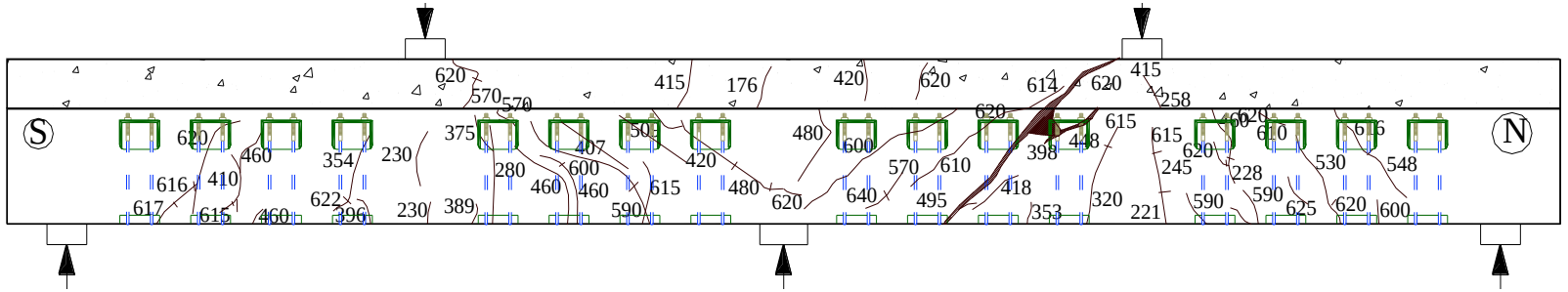

(c) U2.5-0.6

Fig. 5-Typical crack patterns and failure of beams according to type of wire rope units.

(Numbers indicate the total load in kN at which crack occurred.)

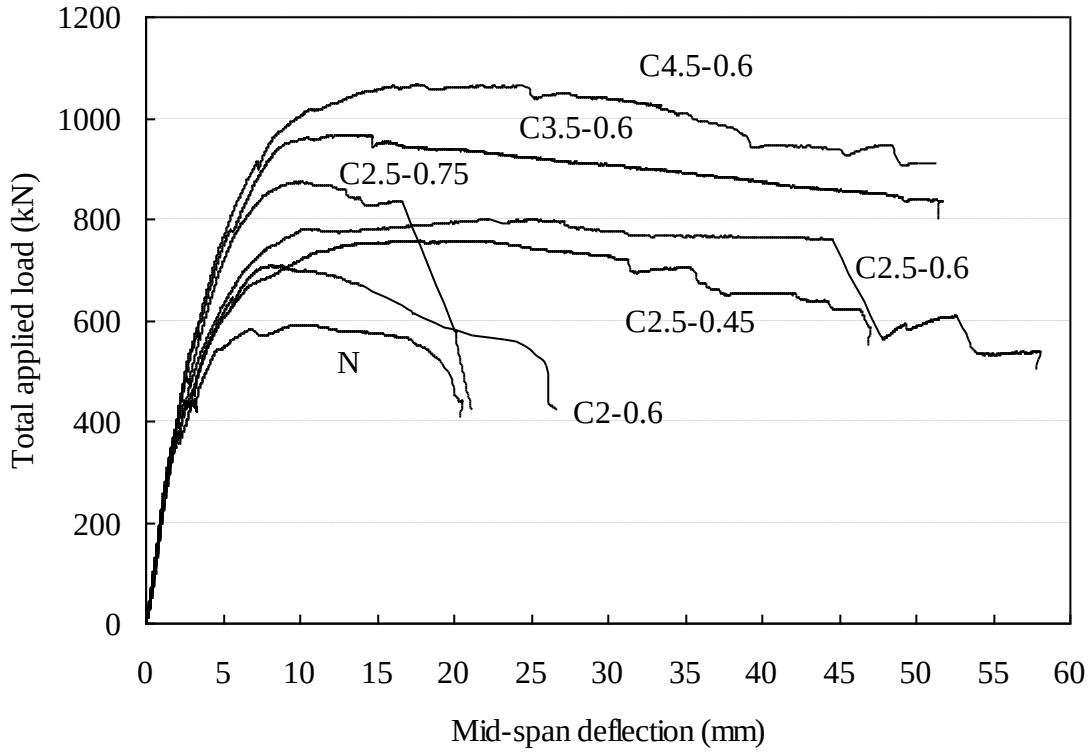

(a) C-series

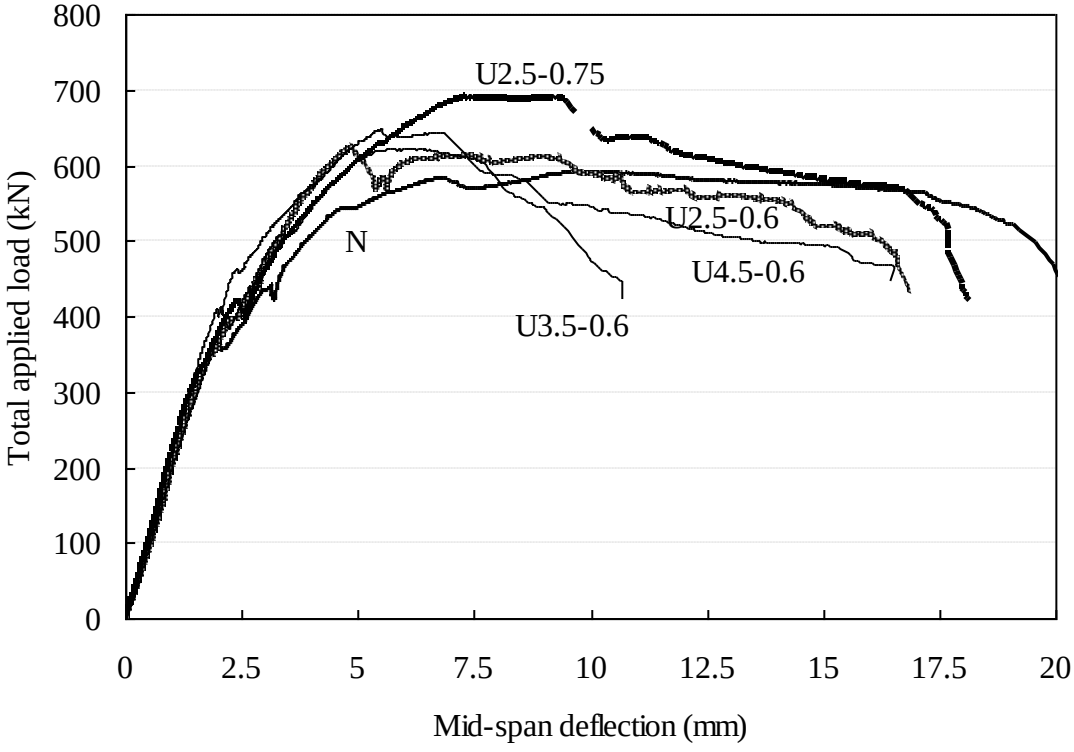

(b) U-series

Fig. 6–Mid-span deflection against total load.

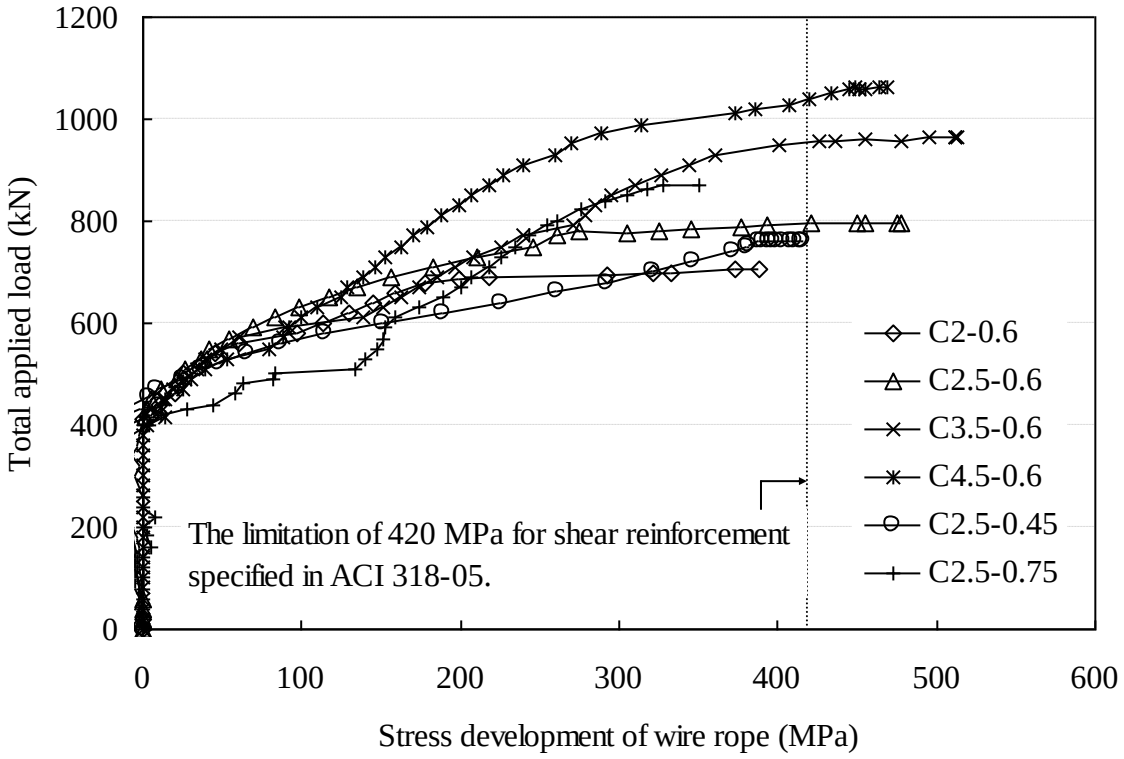

(a) C-series

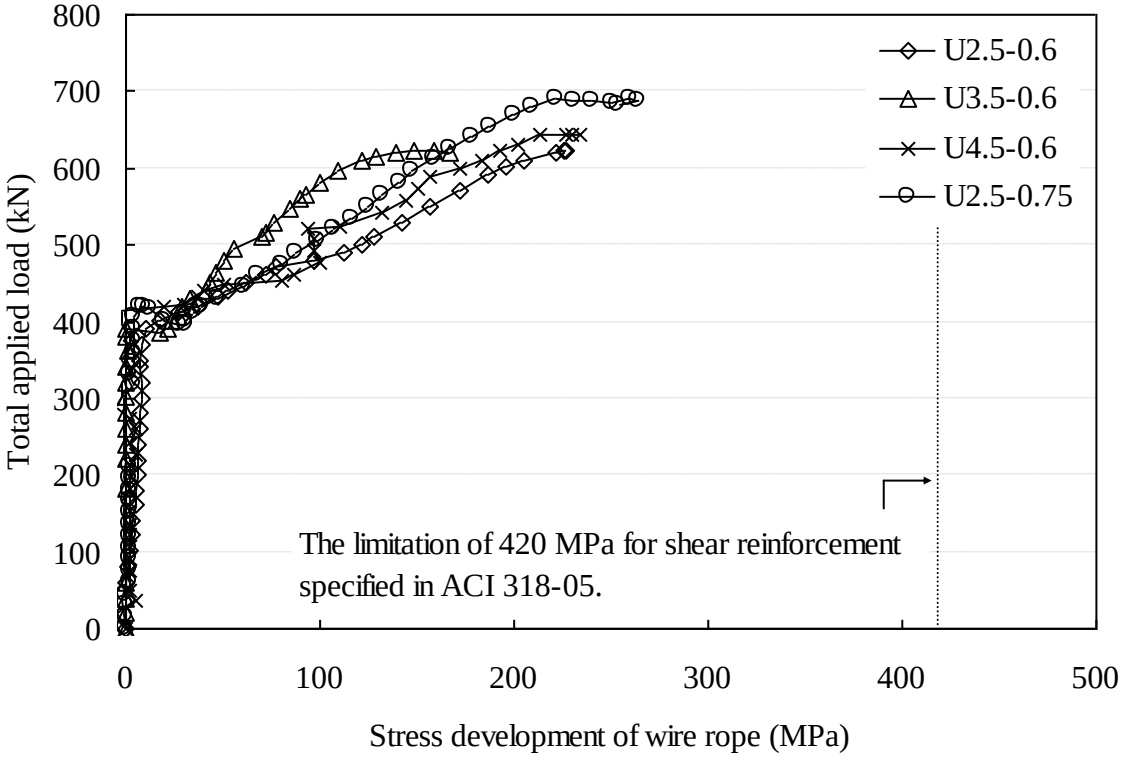

(b) U-series

Fig. 7–Stress development in wire ropes against total load.

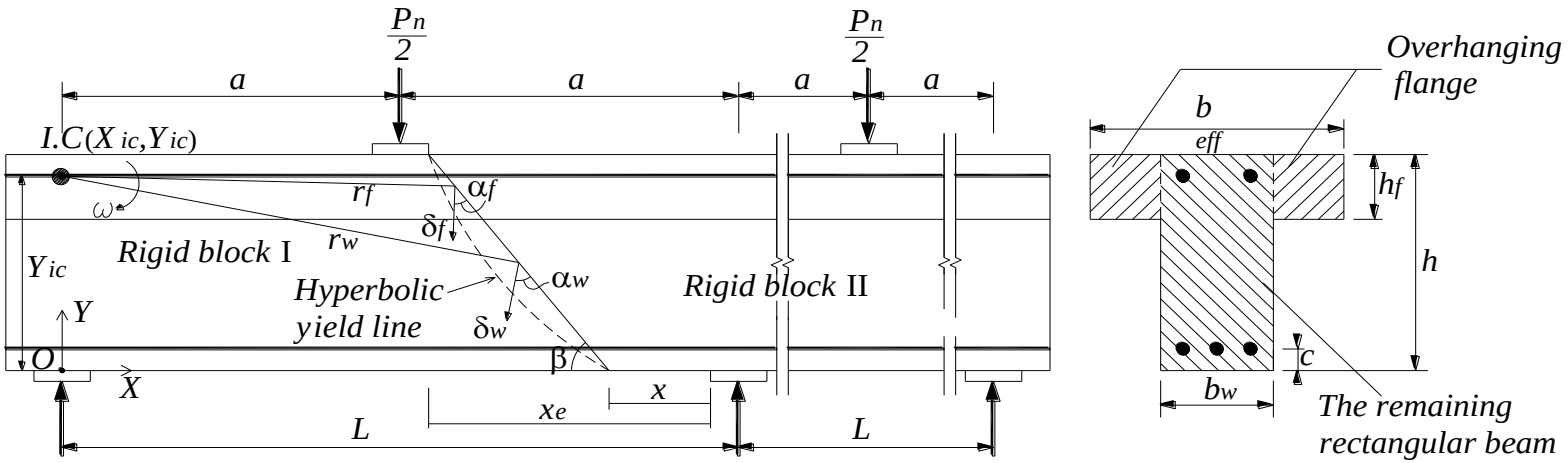

(a) Concrete blocks and hyperbolic yield line

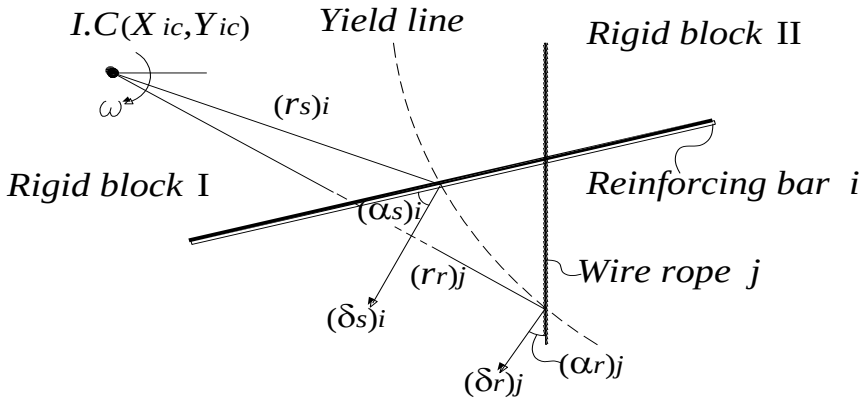

(b) Reinforcing bar and wire rope crossing yield line

Fig. 8–Idealized failure mechanism for two-span continuous T-beams.